Structural response of 20-foot shipping containers during vented hydrogen deflagrations

Trygve Skjold [a,b], Helene Hisken [a], Laurence Bernard [a,b,c] and Arve Grønsund Hanssen [d]
[a] Gexcon, Bergen, Norway
[b] University of Bergen, Bergen, Norway
[c] Air Liquide, Paris Innovation Campus, France
[d] Impetus Afea, Flekkefjord, Norway

1 Introduction

It is common practice to install equipment for hydrogen energy applications in shipping containers. Fires and explosions represent a significant hazard for such installations [1], and specific measures are generally required for reducing the risk to a tolerable level [2]. An adequately designed explosion venting protective system can be an effective means of mitigating the consequences of hydrogen deflagrations in confined systems [3]. Whereas empirical correlations for the design of explosion venting systems in international standards, such as EN 14994 [4] and NFPA 68 [5], focus on the maximum reduced explosion pressure, it is equally important to consider the structural response and integrity of the enclosure. The dynamic response of the structure is particularly relevant for relatively weak structures, such as buildings and containers.

Pressure-impulse (P-I) diagrams indicate combinations of pressure loads and impulse that cause a specific level of damage to a given structure [6-7]. P-I curves divide the P-I diagram into distinct regions, such as negligible damage, moderate damage and failure. Fig. 1 illustrates a classical P-I curve for an ideal blast load where a curved line connects the pressure and impulse asymptotes. This paper explores the possibility of deriving empirical P-I curves from pressure-time histories measured in full-scale vented hydrogen deflagration experiments as a novel method for estimating the structural response of 20-foot containers subjected to the loading from vented hydrogen deflagrations.

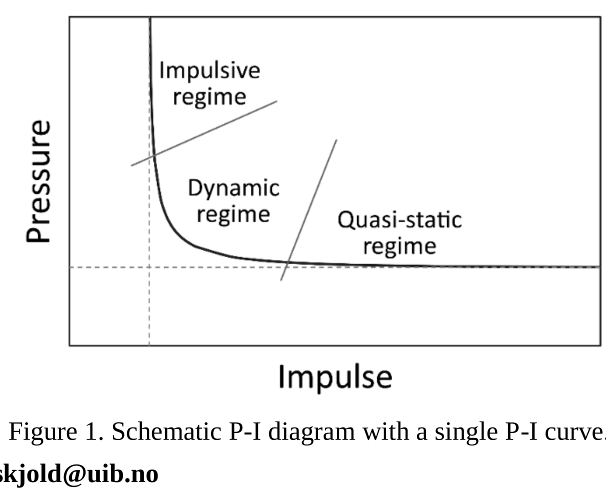

Figure 1. Schematic P-I diagram with a single P-I curve.

Correspondence to: trygve.skjold@uib.no

Several parameters influence the P-I diagram, including pulse shape, the rise time of the load, plasticity, damping and vessel burst [6-7]. In the *impulsive loading regime*, the load duration is short relative to the response time of the system. In the *quasi-static loading regime*, the duration of the load is significantly longer than the response time. The structural response in the *dynamic loading regime* is more complex and significantly influenced by the profile of the load history. P-I diagrams are often derived for idealised load profiles, such as blast loading or impact loading. Baker *et al*. [6] pointed out that the typical structural loading caused by internal gas or dust explosions differ significantly from the loading produced by condensed explosives. Ideal blast waves from condensed explosives and other detonations have zero rise time and near exponential decay [6-9]. Pressure-time histories generated by vented deflagrations, on the other hand, will typically have finite rise time, relatively complex pulse shape, and may exhibit multiple pressure peaks. Due to the resonance between the rate of loading and the natural frequency of the structure, loading with finite rise time is more severe than loading with zero rise time [6].

2 Experiments

Skjold *et al*. [3] describe the background for the HySEA project, the experimental procedures, and the overall results from 66 vented hydrogen deflagration experiments with 20-foot containers. Eight piezoelectric sensors measured pressure in different locations inside the enclosures, and two Laser displacement sensors measured the dynamic deflection of the container walls. To investigate the structural response of a quasi-static internal pressure load, test no. 70 (T-70) was performed with a closed container, i.e. no vent openings, and a low reactivity mixture: 12 vol.% hydrogen in air. The natural frequency of the container walls is about 15-17 Hz [10-11]. Hence, the duration of a quasi-static pressure load had to be significantly longer than 60 milliseconds. In T-70, the confined deflagration maintained a near constant pressure of approximately 0.3 bar for about one second. Although some leakage occurred, the doors remained closed. This paper is primarily concerned with selected results from the measurements of internal pressures loads and the corresponding deflection of the container walls: average maximum reduced explosion pressure P_m, average maximum rate of pressure rise $(\mathrm{d}P/\mathrm{d}t)_m$, average pressure impulse I_m, average maximum deflection D_m and average permanent deformation D_p. Fig. 2 shows some of the containers before and after testing [11].

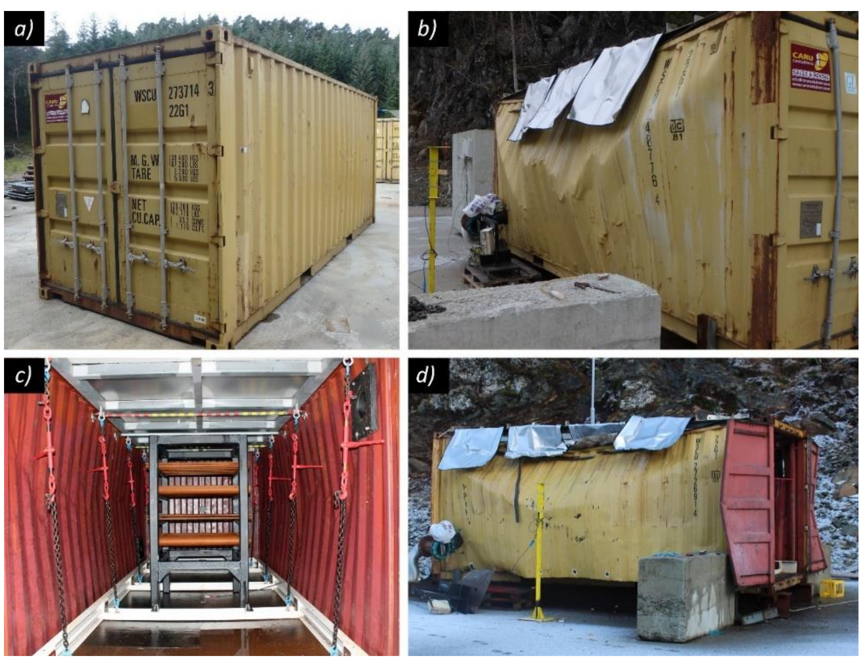

Figure 2. 20-foot shipping containers.

3 Results

Skjold *et al.* [3] summarise the overall results from the 66 vented deflagration tests. Skjold [10-11] describes the processing of the experimental data and Skjold [11] presents detailed plots from each test. The relatively complex shape of the pressure-time histories from the vented deflagrations in the present study complicated the analysis significantly, compared to idealised load profiles with zero rise time that are representative for ideal blast loading [8-9]. In particular, it was not straightforward to determine unambiguous values for impulse for tests with multiple pressure peaks, and the maximum deflection measured in some of the experiments is probably the result of repeated loading at a frequency close to the natural frequency of the corrugated sidewalls of the container, i.e. approximately 15-17 Hz.

Fig. 3 illustrates the correlation between permanent deformation D_p and the parameters P_m, I_m, $(\mathrm{d}P/\mathrm{d}t)_m$ and D_m. Since most of the twelve containers were used in several tests, permanent deformation from previous experiments represents a significant source of uncertainty in the results. Fig. 4 illustrates the correlation between the average maximum (instantaneous) deflection D_m and the parameters P_m, I_m, $(\mathrm{d}P/\mathrm{d}t)_m$ and D_p. The error bars in Figs. 3-4 indicate the variation from the lowest to the highest values measured during each test. Fig. 5 shows examples of empirical P-I diagrams for 20-foot shipping containers, where the damage criteria, i.e. the P-I curves, are based on specific levels of permanent deformation. Attempts at correlating the accumulated permanent deformation observed for consecutive tests with the same container against the same parameters did not produce P-I diagrams with the same level of consistency as Fig. 5.

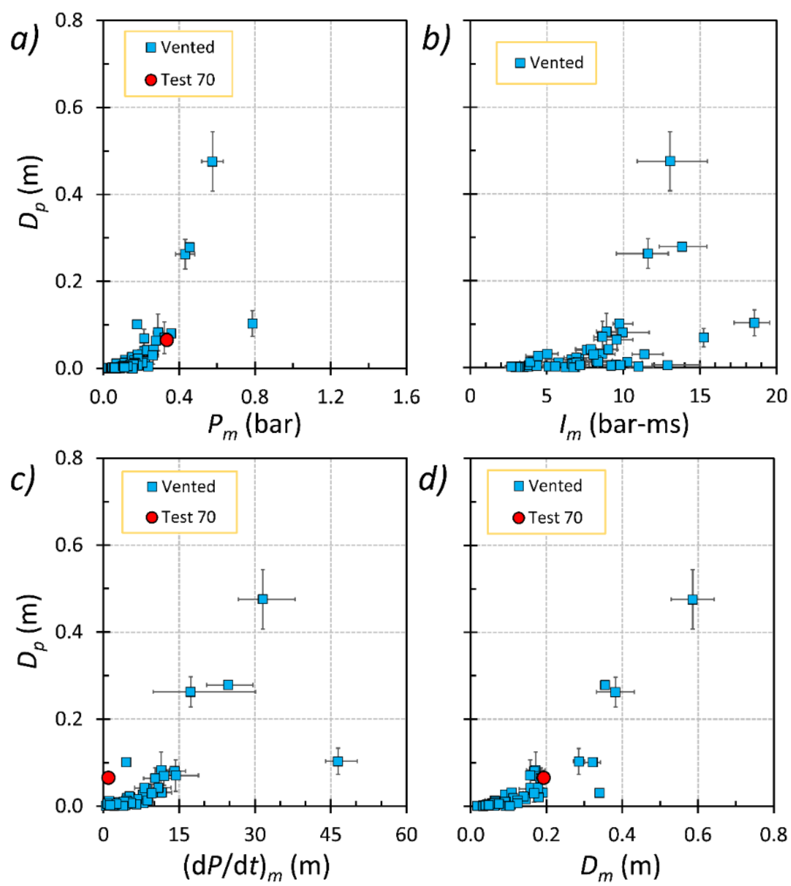

Figure 3. Influence of selected parameters on average permanent deformation D_p.

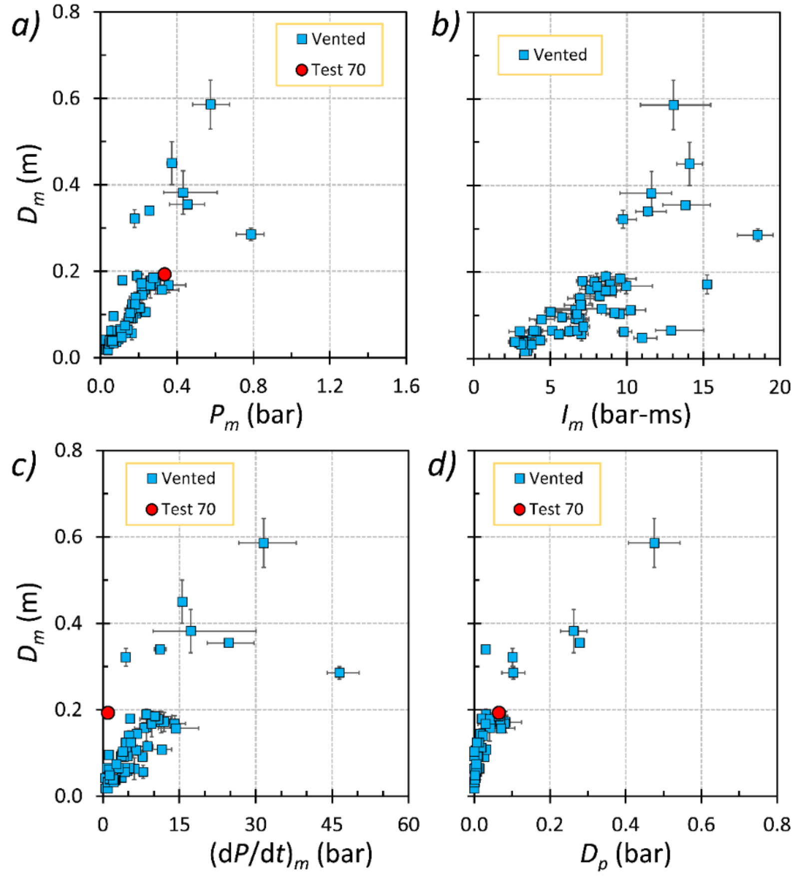

Figure 4. Influence of selected parameters on the average maximum deflection D_m.

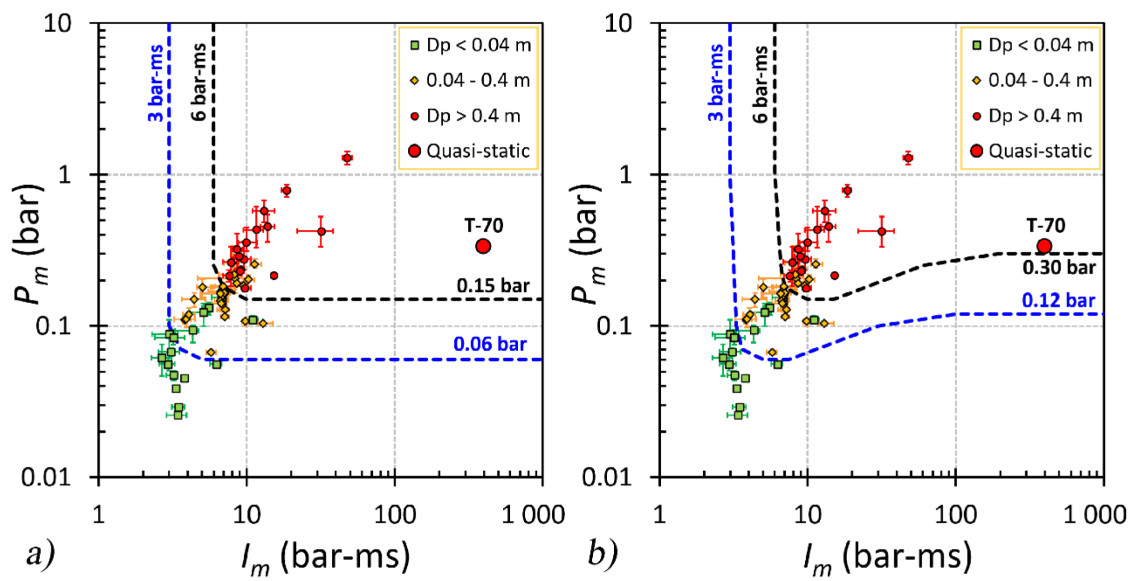

Figure 5. Empirical pressure-impulse diagrams for 20-foot shipping containers.

4 Discussion

It was not straightforward to define unambiguous damage categories for constructing the empirical P-I curves in Fig. 5. Relevant parameters for characterising the structural damage include D_m, D_p, and whether the container ruptured. The values for $(\mathrm{d}P/\mathrm{d}t)_m$ are very sensitive to the procedure used for data processing [10-11], and the influence of this parameter on D_m and D_p differs significantly between and the quasi-static test (T-70) and the tests with venting. Hence, $(\mathrm{d}P/\mathrm{d}t)_m$ was not used for the construction of P-I diagrams. Since the maximum (instantaneous) displacement D_m can be quite sensitive to resonance phenomena, the degree of permanent deformation D_p was the criterion selected for constructing the P-I curves in Fig. 5. The category $D_p > 0.4$ m includes all the tests there the container ruptured.

Apart from T-70, the data points in Fig. 5 appear to be located within the dynamic loading regime (Fig. 1). Hence, the profiles of the load histories influence the dynamic response of the structure. Fig. 5a shows a simplified P-I diagram with P-I curves that would be representative for ideal blast loads with zero rise time. Fig. 5b illustrates a modified version of the diagram that is more consistent with the expected structural behaviour for loading with finite rise time [6]. The complex shape of the pressure-time histories from the vented hydrogen deflagrations introduces significant uncertainty in the analysis and may limit the general applicability of the proposed P-I diagrams for design purposes.

In principle, it should be possible to complement the experimental results from the HySEA project with data from computational fluid dynamics (CFD) and finite element (FE) simulations of vented deflagrations [12]. However, the results from the two blind-prediction benchmark studies conducted as part of the HySEA project demonstrate that it is not straightforward to simulate vented hydrogen deflagrations in 20-foot shipping containers with internal congestion [13-14]. As such, it is necessary to improve the predictive capabilities of advanced consequence models for vented hydrogen deflagrations. It is particularly important to improve the modelling of flame acceleration in highly congested geometries and to implement models that describe the opening of realistic explosion venting devices with sufficient accuracy [14].

Safe design of container-based installations for hydrogen energy applications should consider the hazard of projectiles generated from vented deflagrations. The experiments with 20-foot shipping containers on the HySEA project demonstrated that the container doors do not represent suitable explosion venting devices [3,11]. Properly installed and certified explosion venting devices should not represent a hazard [15], but it may also be necessary to secure structural elements such as louvre panels and fans for natural or forced ventilation. Finally, explosion protection by venting is only effective for deflagrations, not detonations.

4 Conclusions

Pressure-impulse (P-I) diagrams are often used for assessing the damage of structural components. This paper describes the construction of empirical P-I diagrams for the structural response of 20-foot shipping containers subjected to internal pressure loads generated by vented hydrogen deflagrations [3,11]. There is significant uncertainty associated with the results, primarily due to the inherently complex nature of the pressure loading and the fact that many of the experiments inevitably used containers with permanent deformation from previous tests. Nevertheless, the fact that most of the experimental data points fall within well-defined areas suggests that the proposed P-I diagrams may be useful for design purposes.

Acknowledgements

The HySEA project receives funding from the Fuel Cells and Hydrogen 2 Joint Undertaking under grant agreement No. 671461. This Joint Undertaking receives support from the European Union's Horizon 2020 research and innovation programme and the United Kingdom, Italy, Belgium and Norway.

References

[1] Skjold T, Souprayen C, Dorofeev S. (2018). Fires and explosions. Prog. Energy Combust. Sci. 64: 2-3.

[2] Skjold T, Siccama D, Hisken H, Brambilla A, Middha P, Groth KM, LaFleur AC (2017). 3D risk management for hydrogen installations. Int. J. Hydrog. Energy, 42: 7721-7730.

[3] Skjold T, Hisken H, Lakshmipathy S, Atanga G, van Wingerden M, Olsen KL, Holme MN, Turøy NM, Mykleby M, van Wingerden K. (2018). Vented hydrogen deflagrations in containers: effect of congestion for homogeneous and inhomogeneous mixtures. Int. J. Hydrog. Energy, 44: 8819-8832.

[4] EN 14994 (2007). Gas explosion venting protective systems. European Committee for Standardization (CEN), Brussels: 30 pp.

[5] NFPA 68 (2018). Standard on explosion protection by deflagration venting. National Fire Protection Association (NFPA), Quincy, Massachusetts.

[6] Baker WE, Cox PA, Westine PS, Kulesz JJ and Strehlow, RA (1983). Explosion hazards and evaluation, Elsevier, Amsterdam.

[7] Krauthammer T (2008). Modern protective structures. CRC Press, Boca Raton.

[8] Friedlander FG (1946). The diffraction of sound pulses I. Diffraction by a semi-infinite plate. Proc. Royal Soc. Lond. A, 186, 1946: 322-344.

[9] Dewey JM (2010). The shape of the blast wave: studies of the Friedlander equation. Proc. 21 MABS, Jerusalem, 3-8 October 2010: 9 pp.

[10] Skjold T (2018). Vented hydrogen deflagrations in 20-foot ISO containers. Proc. 12 ISHPMIE, Kansas City, 12-17 August 2018: 823-846.

[11] Skjold T (2018). Experimental investigation of vented hydrogen deflagrations in containers: homogeneous and inhomogeneous mixtures. Report HySEA-D2-08-2018: 638 pp.

[12] Atanga G, Lakshmipathy S, Skjold T, Hisken H., Hanssen AG (2019). Structural response for vented hydrogen deflagrations: coupling CFD and FE tools. Int. J. Hydrog. Energy, 44: 8893-8903.

[13] Skjold T, Hisken H, Lakshmipathy S, Atanga G, Carcassi M, Schiavetti M, Stewart JR, Newton A, Hoyes JR, Tolias IC, Venetsanos AG, Hansen OR, Geng J, Huser A, Helland S, Jambut R, Ren K, Kotchourko A, Jordan T, Daubech J, Lecocq G, Hanssen AG, Kumar C, Krumenacker L, Jallais S, Miller D, Bauwens CR (2019). Blind-prediction: estimating the consequences of vented hydrogen deflagrations for homogeneous mixtures in 20-foot ISO containers. Int. J. Hydrog. Energy, 44: 8997-9008.

[14] Skjold T, Hisken H, Bernard L, Mauri L, Atanga G, Lakshmipathy S, Pérez ML, Carcassi M, Schiavetti M, Rao VCM, Sinha A, Tolias IC, Giannissi SG, Venetsanos AG, Stewart JR, Hansen, OR, Kumar C, Krumenacker L, Laviron F, Jambut R, Huser A (2018). Blind-prediction: estimating the consequences of vented hydrogen deflagrations for inhomogeneous mixtures in 20-foot ISO containers. Proc. 12 ISHPMIE, Kansas City, 12-17 August 2018: 875-898.

[15] EN 14797 (2006). Explosion venting devices. European Committee for Standardization (CEN), Brussels: 30 pp.